



**HAL**  
open science

## Versatility and adaptative behaviour of the $P^N$ chelatingligandMeDalphoswithingold( $i$ ) $\pi$ complexes

Miquel Navarro, Alberto Toledo, Sonia Mallet-Ladeira, E. Daiann Sosa Carrizo, Karinne Miqueu, Didier Bourissou

### ► To cite this version:

Miquel Navarro, Alberto Toledo, Sonia Mallet-Ladeira, E. Daiann Sosa Carrizo, Karinne Miqueu, et al.. Versatility and adaptative behaviour of the  $P^N$ chelatingligandMeDalphoswithingold( $i$ ) $\pi$  complexes. Chemical Science, 2020, 11 (10), pp.2750-2758. 10.1039/C9SC06398F . hal-03005626v2

**HAL Id: hal-03005626**

**<https://hal.science/hal-03005626v2>**

Submitted on 23 Mar 2021

**HAL** is a multi-disciplinary open access archive for the deposit and dissemination of scientific research documents, whether they are published or not. The documents may come from teaching and research institutions in France or abroad, or from public or private research centers.

L'archive ouverte pluridisciplinaire **HAL**, est destinée au dépôt et à la diffusion de documents scientifiques de niveau recherche, publiés ou non, émanant des établissements d'enseignement et de recherche français ou étrangers, des laboratoires publics ou privés.

**Versatility and adaptative behaviour of the  $P^N$  chelating ligand *MeDalphos* with  $gold(i)\pi$  complexes**

Miquel Navarro, Alberto Toledo, Sonia Mallet-Ladeira, E. Daiann Sosa Carrizo, Karinne Miqueu, Didier Bourissou

► **To cite this version:**

Miquel Navarro, Alberto Toledo, Sonia Mallet-Ladeira, E. Daiann Sosa Carrizo, Karinne Miqueu, et al. Versatility and adaptative behaviour of the  $P^N$  chelating ligand *MeDalphos* with  $gold(i)\pi$  complexes. *Chemical Science*, The Royal Society of Chemistry, 2020, 11 (10), pp.2750-2758. 10.1039/C9SC06398F . hal-02999887


**HAL Id: hal-02999887**

**<https://hal.archives-ouvertes.fr/hal-02999887>**

Submitted on 23 Nov 2020

**HAL** is a multi-disciplinary open access archive for the deposit and dissemination of scientific research documents, whether they are published or not. The documents may come from teaching and research institutions in France or abroad, or from public or private research centers.

L'archive ouverte pluridisciplinaire **HAL**, est destinée au dépôt et à la diffusion de documents scientifiques de niveau recherche, publiés ou non, émanant des établissements d'enseignement et de recherche français ou étrangers, des laboratoires publics ou privés.

Cite this: *Chem. Sci.*, 2020, **11**, 2750 All publication charges for this article have been paid for by the Royal Society of Chemistry

# Versatility and adaptative behaviour of the P<sup>^</sup>N chelating ligand MeDalphos within gold(I) $\pi$ complexes<sup>†</sup>

Miquel Navarro,<sup>a</sup> Alberto Toledo,<sup>a</sup> Sonia Mallet-Ladeira,<sup>b</sup> E. Daiann Sosa Carrizo,<sup>c</sup> Karinne Miqueu<sup>c</sup> and Didier Bourissou<sup>a\*</sup>

The hemilabile P<sup>^</sup>N ligand MeDalphos enables access to a wide range of stable gold(I)  $\pi$ -complexes with unbiased alkenes and alkynes, as well as electron-rich alkenes and for the first time electron-poor ones. All complexes have been characterized by multi-nuclear NMR spectroscopy and whenever possible, by X-ray diffraction analyses. They all adopt a rare tricoordinate environment around gold(I), with chelation of the P<sup>^</sup>N ligand and side-on coordination of the alkene, including the electron-rich one, 3,4-dihydro-2H-pyran. The strength of the N  $\rightarrow$  Au coordination varies significantly in the series. It is the way the P<sup>^</sup>N ligand accommodates the electronic demand at gold, depending on the alkene. Comparatively, when the chelating P<sup>^</sup>P ligand (*ortho*-carboranyl)(PPh<sub>2</sub>)<sub>2</sub> is used, gold(I)  $\pi$ -complexes are only isolable with unbiased alkenes. The bonding situation within the gold(I) P<sup>^</sup>N  $\pi$ -complexes has been thoroughly analyzed by DFT calculations supplemented by Charge Decomposition Analyses (CDA), Natural Bond Orbital (NBO) and Atoms-in-Molecules (AIM) analyses. Noticeable variations in the donation/back-donation ratio, C=C weakening, alkene to gold charge transfer and magnitude of the N  $\rightarrow$  Au coordination were observed. Detailed examination of the descriptors for the Au/alkene interaction and the N  $\rightarrow$  Au coordination actually revealed intimate correlation between the two, with linear response of the MeDalphos ligand to the alkene electronics. The P<sup>^</sup>N ligand displays non-innocent and adaptative character. The isolated P<sup>^</sup>N gold(I)  $\pi$ -complexes are reactive and catalytically relevant, as substantiated by the chemo and regio-selective alkylation of indoles.

Received 17th December 2019  
Accepted 31st January 2020

DOI: 10.1039/c9sc06398f

rsc.li/chemical-science

## Introduction

For a long time, gold was considered to be “the noblest of all metals”<sup>1</sup> and too chemically inert to be used in catalysis. However, since the discovery of the ability of gold to activate  $\pi$ -bonds towards nucleophilic addition, homogenous gold catalysis has emerged as a very powerful tool in organic synthesis.<sup>2</sup> A large number of useful transformations such as the addition of oxygen-, nitrogen- and carbon-nucleophiles to CC multiple bonds, rearrangements and cycloaddition reactions have been

developed.<sup>3</sup> All these catalytic reactions usually involve the initial  $\pi$ -coordination of a CC multiple bond to gold. Consequently, the isolation of gold  $\pi$ -complexes has received considerable attention.<sup>4-6</sup> The prepared compounds serve as models for the transient species and their study provide valuable insight into the factors governing the catalytic transformations. Over the last 15 years, a number of cationic dicoordinate gold(I)  $\pi$ -complexes have been isolated and characterized with *N*-heterocyclic carbenes (NHCs) or phosphines as ancillary ligands, and electron-unbiased alkenes such as styrene and hex-1-ene (Fig. 1).<sup>4,5</sup> A few complexes have also been reported with electron-rich alkenes, such as enamines and enol ethers, for which coordination tends to slip from side-on to terminal.<sup>7</sup> In addition, *N*-based chelating ligands have been occasionally found to form stable tricoordinate gold(I)  $\pi$ -complexes.<sup>8</sup> Nonetheless, the number and variety of known  $\pi$ -alkene gold complexes are still limited. Tricoordinate species remain very scarce<sup>9</sup> and to the best of our knowledge, gold  $\pi$ -complexes featuring electron-poor alkenes are hitherto known.

With the aim to advance further our knowledge on these key reactive intermediates in gold chemistry, we aimed in this work to address the following question: is it possible for a unique ligand to accommodate the  $\pi$ -coordination of a wide range of

<sup>a</sup>CNRS/Université Paul Sabatier, Laboratoire Hétérochimie Fondamentale et Appliquée (LHFA, UMR 5069), 118 Route de Narbonne, 31062 Toulouse Cedex 09, France. E-mail: dbouriss@chimie.ups-tlse.fr

<sup>b</sup>Institut de Chimie de Toulouse (FR 2599), 118 Route de Narbonne, 31062 Toulouse Cedex 09, France

<sup>c</sup>CNRS/Université de Pau et des Pays de l'Adour, Institut des Sciences Analytiques et de Physico-Chimie pour l'Environnement et les Matériaux (IPREM UMR 5254), Hélioparc, 2 Avenue du Président Angot, 64053 Pau Cedex 09, France

<sup>†</sup> Electronic supplementary information (ESI) available: Experimental and computational details, analytical data and NMR spectra. CCDC 1967901 (3), 1967904 (5), 1967902 (6), 1967903 (7), 1967905 (9) and 1967906 (13g). For ESI and crystallographic data in CIF or other electronic format see DOI: 10.1039/c9sc06398f



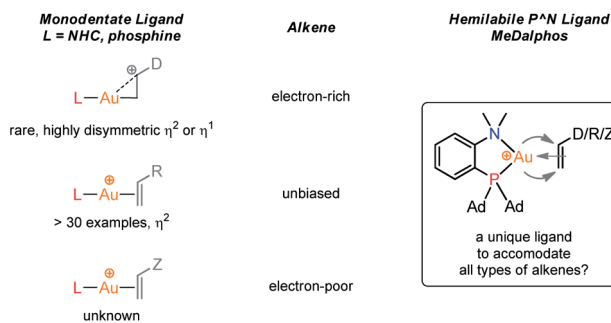


Fig. 1 Alkene gold(i) complexes (D = electron-donating, Z = electron-withdrawing substituents).

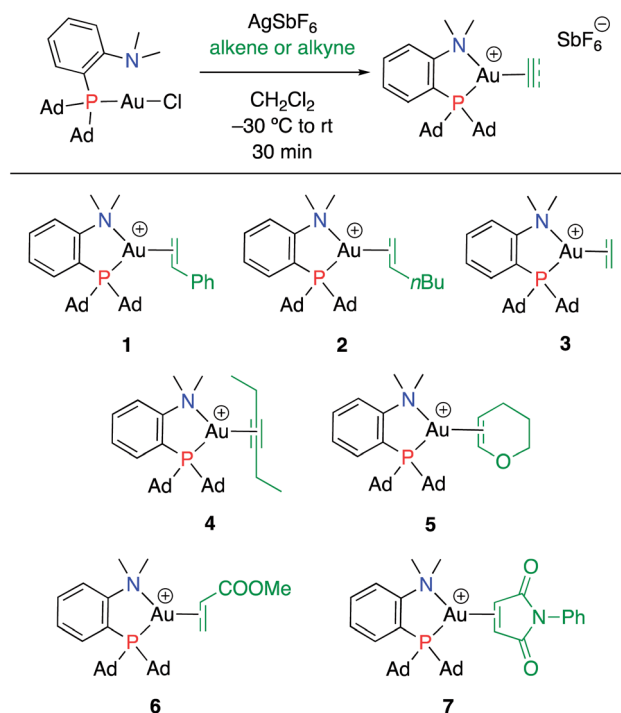
alkenes at gold, *i.e.* unbiased as well as electron-rich and electron-poor alkenes? To this end, we envisioned to take advantage of the higher modularity of bifunctional ligands to find a proper balance in stability/reactivity. Indeed, the alkenes should bind tightly enough to gold to form stable complexes, but the coordination should not result in too strong activation of the  $\pi$ -system to induce oligomerization by polyaddition.

Our recent isolation of tridentate gold(i) complexes of styrene with  $P^*P$  chelating and  $P^*N$  hemilabile ligands<sup>10</sup> prompted us to screen a range of other  $\pi$ -systems. Gratifyingly, stable gold(i)  $\pi$ -complexes were found to be readily accessible with different unbiased alkenes and alkynes such as hex-1-ene, ethylene and hex-3-yne, as well as 3,4-dihydro-2H-pyran (DHP) as electron-rich alkene, and methylacrylate (MA) and *N*-phenylmaleimide (NPM) as electron-poor alkenes. These results are reported hereafter, along with detailed characterization and analysis of the bonding situation by experimental and computational means. This study unveils the faculty of the  $P^*N$  ligand to respond and accommodate the electron demand at gold by weakening/strengthening the  $N \rightarrow Au$  interaction.

## Results and discussion

### Synthesis and characterization of ( $P^*N$ )Au(i) $\pi$ -complexes

Treatment of MeDalpos gold(i) chloride with  $AgSbF_6$  in the presence of an excess (3 equiv.) of alkene or alkyne proved to be a general entry to gold(i)  $\pi$ -complexes, as illustrated by the preparation of the series of complexes 1–7 (Scheme 1).<sup>11</sup> The reactions were conveniently monitored by <sup>31</sup>P NMR spectroscopy. Filtration of the reaction mixtures through short pads of Celite followed by washing with  $Et_2O$  afforded the pure gold(i)  $\pi$ -complexes 1–6 in good yields (50–89%). Only complex 7 proved too unstable to be isolated. Since decomposition occurred upon filtration, it was characterized in the presence of excess of *N*-phenylmaleimide without further purification. Complexes 1–6 are air stable solids. Their <sup>1</sup>H and <sup>13</sup>C NMR spectra display a new set of well-defined signals for the alkene/alkyne (distinct from those of the free  $\pi$ -system). No chemical exchange was observed between the coordinated and free alkene/alkyne within the NMR time-scale. No sign of alkene/alkyne dissociation was detected either under vacuum.



Scheme 1 Synthesis of gold(i)  $\pi$ -complexes 1–7.

Coordination to gold(i) induces a marked upfield shift (with exception of complex 5 that shows a downfield shift) of the <sup>1</sup>H and <sup>13</sup>C NMR signals with respect to the free alkene/alkyne (Table 1 and S2†).<sup>11</sup> These shift differences reach up to 2.13 ppm in <sup>1</sup>H NMR and 65 ppm in <sup>13</sup>C NMR spectroscopy, suggesting substantial gold  $\rightarrow \pi^*$  back-donation (see below). Another conspicuous feature of all  $\pi$ -complexes is the sizeable downfield shift of the  $N(CH_3)_2$  <sup>1</sup>H NMR signal, as compared to the (MeDalpos) AuCl precursor. Interestingly, the magnitude of the <sup>1</sup>H NMR downfield shift of the  $N(CH_3)_2$  signal seems to correlate with the electronic properties of the  $\pi$ -system:  $\Delta\delta$

Table 1 Selected <sup>1</sup>H, <sup>13</sup>C and <sup>31</sup>P NMR data ( $\delta$  in ppm) for the  $\pi$ -alkene gold(i) complexes 1–3 and 5–7<sup>a</sup>

| $\delta^1H$    | $H_{alkene}$ | 7.76  | 6.03 | 5.66  | 4.10 | 4.61 | 4.68 |
|----------------|--------------|-------|------|-------|------|------|------|
|                |              | 4.78  | 4.33 | 3.94  | 4.35 | 4.23 | 5.67 |
|                | $H_{NMe_2}$  | 2.74  | 3.09 | 3.01  | 3.14 | 3.25 | 3.44 |
| $\delta^{13}C$ | $C_{alkene}$ | 2.71  | 2.82 | 2.98  | 3.07 | 3.07 | 3.33 |
|                |              | 144.1 | 99.9 | 111.1 | 75.0 | 72.5 | 72.4 |
|                | $C_{NMe_2}$  | 76.7  | 66.4 | 75.2  | 68.4 | 68.8 | 68.8 |
| $\delta^{31}P$ |              | 49.5  | 53.0 | 52.5  | 53.9 | 45.9 | 55.4 |
|                |              | 49.3  | 52.8 |       | 53.8 | 55.2 |      |
|                |              | 56.5  | 57.3 | 58.1  | 58.8 | 63.2 | 65.3 |

<sup>a</sup> All data recorded in  $CD_2Cl_2$ . Data for the styrene complex 1 from ref. 10.



increases from 0.15 ppm for the DHP complex **5** (electron-rich alkene) to 0.82 ppm for the NPM complex **7** (electron-poor alkene) while complexes **1–4** with unbiased alkenes/alkyne exhibit intermediate values ( $\Delta\delta \sim 0.5$  ppm). Similar trends are observed in  $^{13}\text{C}$  NMR [the  $\text{N}(\text{CH}_3)_2$  signals shift from 49.4 for DHP to 55.3 ppm for NPM] as well as  $^{31}\text{P}$  NMR spectroscopy (the signal shifts from 56.5 ppm for DHP to 65.3 ppm for NPM). These observations suggest that the  $\text{P}^\wedge\text{N}$  ligand adjusts its coordination to gold depending on the electronics of the  $\pi$ -system, and that NMR spectroscopy is a sensitive reporter for this adaptive behavior.

Single crystals of complexes **3**, **5**, **6** and **7** suitable for X-ray diffraction analysis were obtained.<sup>11</sup> Overall, the four complexes adopt similar structures in the solid state (Fig. 2): the  $\text{SbF}_6^-$  counter anion is ion separated and the  $\text{P}^\wedge\text{N}$  ligand chelates gold. In all complexes, the gold centre is in trigonal planar environment and the alkene sits in the coordination plane of gold despite the ensuing steric shielding.<sup>12</sup> This arrangement ensures optimal overlap between the HOMO of the

$[(\text{P}^\wedge\text{N})\text{Au}^+]$  fragment (in-plane d-type orbital) and the  $\pi^*$ (alkene) orbital. The presence of substantial  $\text{Au} \rightarrow$  alkene back-donation is also apparent from the elongation of the  $\text{C}=\text{C}$  bond upon coordination to gold (by  $\sim 0.06$  Å compared to the free alkene). For comparison with related gold(I) alkene complexes, see Table S4.†<sup>11</sup> In all cases, the alkene is  $\eta^2$ -coordinated to gold, and complexes **3**, **6** and **7** present quasi-symmetric structures with almost identical  $\text{Au}-\text{C}$  bond lengths (Table 2). As expected from the electron-rich and polarized character of DHP, complex **5** adopts a slipped coordination mode ( $\text{Au}-\text{C}$  2.193(3) and 2.276(3) Å), but the alkene remains  $\eta^2$ -coordinated. This situation contrasts with the highly dissymmetric structures (terminal  $\sigma$ -coordination rather than side-on  $\pi$ -coordination) generally observed in the few previously reported gold(I) complexes featuring electron-rich alkenes (Fig. S28†).<sup>7</sup> Within the series of  $\pi$ -complexes **3**, **5**, **6** and **7**, little changes are observed in the  $\text{Au}-\text{P}$  bond length [min.–max. values = 2.3032(2) and 2.3393(3) Å], whereas the  $\text{Au}-\text{N}$  bond length varies from 2.234(6) Å in complex **7** with the most electron-poor alkene NPM, to 2.505(2) Å in complex **5** presenting the most electron-rich alkene DHP. This variation attests the adaptive behavior of the  $\text{P}^\wedge\text{N}$  ligand.<sup>13</sup> The  $\text{N} \rightarrow \text{Au}$  interaction strengthens/weakens to accommodate the electronic demand at gold depending on the alkene.

### Synthesis and characterization of $(\text{P}^\wedge\text{P})\text{Au}(\text{i})$ $\pi$ -complexes

To assess the role of the ancillary ligand on the ability of gold(I) to form stable  $\pi$ -complexes with a variety of alkenes, we then turned to the  $\text{P}^\wedge\text{P}$  chelating *o*-carboranyl diphosphine ligand for which a stable styrene complex (**8**) analogous to the  $\text{P}^\wedge\text{N}$  complex **1** was previously prepared.<sup>10</sup> The  $(\text{P}^\wedge\text{P})\text{AuCl}$  precursor was reacted with  $\text{AgSbF}_6$  in the presence of an excess of ethylene (**9**), DHP (**10**), MA (**11**) and NPM (**12**) in dichloromethane (Scheme 2).<sup>11</sup> The coordination of ethylene to the  $[(\text{P}^\wedge\text{P})\text{Au}^+]$  fragment was readily established thanks to  $^1\text{H}$  NMR spectroscopy: a new singlet appeared at 4.47 ppm, close to that found for the corresponding  $\text{P}^\wedge\text{N}$  ethylene complex **3** (4.10 ppm). Complex **9** was isolated as a white solid in good yield (84%). As for the  $\text{P}^\wedge\text{P}$  styrene complex, no sign of ethylene dissociation was observed either in solution or under vacuum. Complex **9** was characterized by X-ray diffraction, showing the side-on in plane

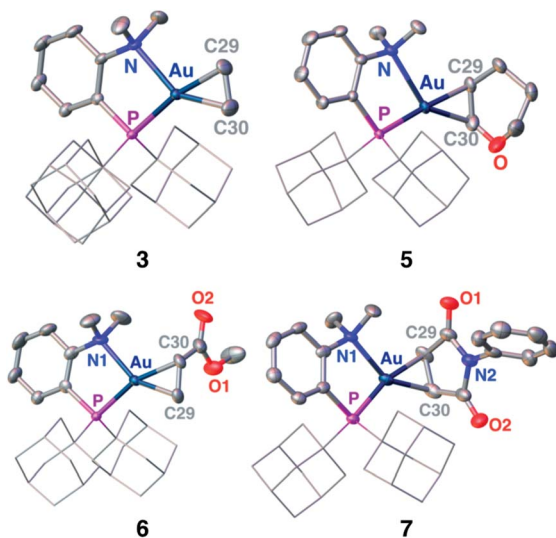


Fig. 2 Molecular structures of complexes **3** (ethylene), **5** (DHP), **6** (MA) and **7** (NPM). Hydrogen atoms, counter anions and solvate molecules are omitted; the adamantyl groups are simplified for clarity.

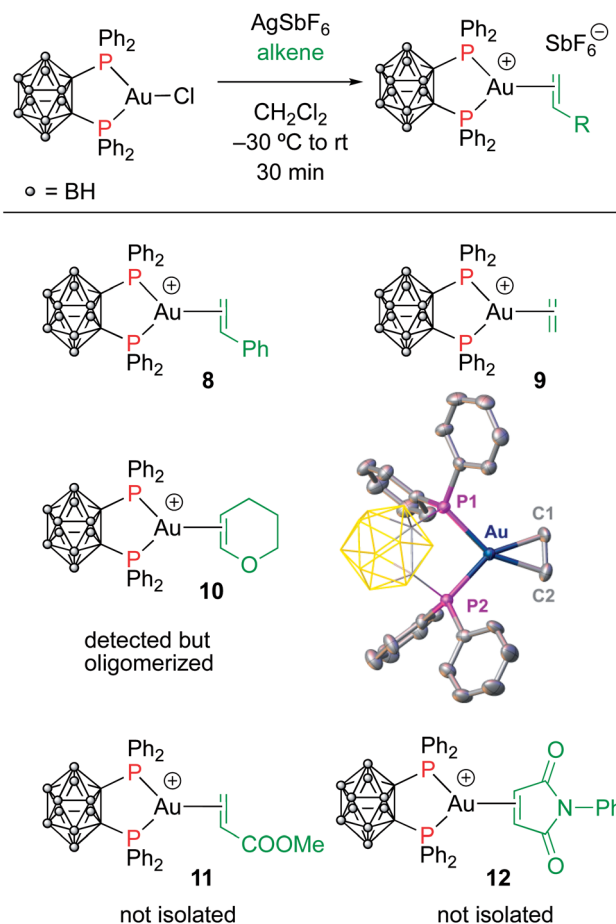
Table 2 Selected bond lengths (Å) for the  $\pi$ -alkene gold(I) complexes **1**, **3**, **5**, **6** and **7**<sup>a</sup>

| Au–P | 2.3032(6) | 2.337(1) | 2.3393(5) | 2.326(1)  | 2.334(2)  |
|------|-----------|----------|-----------|-----------|-----------|
| Au–N | 2.505(2)  | 2.381(4) | 2.306(2)  | 2.275(5)  | 2.234(6)  |
| Au–C | 2.276(3)  | 2.208(5) | 2.141(3)  | 2.114(6)  | 2.133(8)  |
|      | 2.193(3)  | 2.143(5) | 2.149(3)  | 2.155(6)  | 2.136(7)  |
| C=C  | 1.385(5)  | 1.387(8) | 1.387(5)  | 1.406(10) | 1.394(12) |

<sup>a</sup> Data for the styrene complex **1** from ref. 10.







**Scheme 2** Synthesis of the (P<sup>P</sup>) gold(I) complexes **8**–**12**. Molecular structure of complex **9**. Hydrogen atoms, counter anions and solvate molecules are omitted; the carboranyl group is simplified for clarity. Selected bond lengths (Å) and angles (°): Au–P1 2.371(2), Au–P2 2.368(2), Au–C1 2.176(9), Au–C2 2.175(10), C1–C2 1.365(15), P1–Au–P2 91.32(7).

coordination of ethylene. In contrast with that observed with the MeDalphos ligand, electron-rich and electron-poor alkenes did not form stable complexes with the *o*-carboranyl diphosphine. With DHP, complex **10** was detected in small amounts by <sup>1</sup>H NMR spectroscopy at the beginning of the reaction (Fig. S25†), but it rapidly degrades with oligomerization of DHP. Better results were obtained with the electron-poor alkenes MA and NPM. Complexes **11** and **12** formed quantitatively and could be unambiguously characterized by <sup>1</sup>H and <sup>31</sup>P NMR in the presence of an excess of alkene (Fig. S26 and S27†), but attempts at isolation proved unsuccessful due to decomposition. These results highlight the faculty of the heteroleptic P<sup>N</sup> ligand to accommodate all types of alkenes thanks to its adaptive behavior. The *o*-carboranyl diphosphine ligand is apparently less flexible electronically and forms isolable gold(I) π-complexes only with unbiased alkenes.

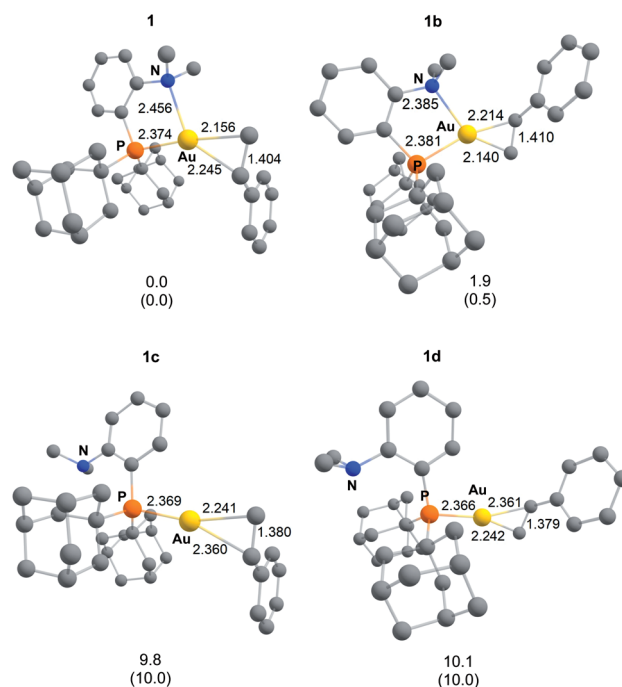
### Theoretical investigation of (P<sup>N</sup>)Au(I) π-complexes

With the aim to better understand the ability of the P<sup>N</sup> ligand to accommodate the π-coordination of a wide range of alkenes

at gold, a detailed computational study was conducted. To the best of our knowledge, very few computational studies have been performed on tridentate gold(I) alkene complexes. The bonding situation within [(2,2'-bipy)Au(ethylene)]<sup>+</sup><sup>8b</sup> was investigated in 2006 and very recently, calculations were carried out on [(phenanthroline)Au(norbornene)]<sup>+</sup> complexes.<sup>14</sup>

**(P<sup>N</sup>)Au(styrene)<sup>+</sup> complex.** DFT calculations were first carried out on the styrene π-complex **1**. Optimizations were performed at the B3PW91/SDD+f(Au),6-31G\*\* (other atoms) level of theory on the real system (with the exact MeDalphos ligand), taking into account solvent effects (by means of the universal solvation model based on solute electron density SMD) but not the SbF<sub>6</sub><sup>−</sup> counter-anion (all complexes adopt discrete ion-pair structures).<sup>11</sup> Four isomers differing in the position of the Ph substituent of the alkene (*cis* to P or N) and in the orientation of the N atom (pointing towards Au or opposite to it) were located on the potential energy surface (Fig. 3 and Table 3). The ground-state structure (referred to as **1**) is consistent with that observed experimentally: the Ph substituent is in *cis* position to the PAD<sub>2</sub> group and the N atom is coordinated to gold. The dicoordinate isomers are 8–10 kcal mol<sup>−1</sup> higher in energy, substantiating the stabilizing effect of P<sup>N</sup> chelating coordination.

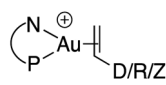
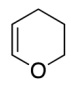
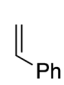
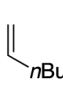
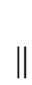
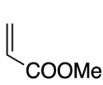
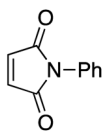
NBO (Natural Bond Orbital), CDA (Charge Decomposition Analysis) and AIM (Atoms-In-Molecules) approaches were used to thoroughly analyse the bonding situation in complex **1** (Table 3), referring to the dicoordinate forms and free alkene when appropriate.<sup>11</sup> Special attention was given to the Au/alkene



**Fig. 3** Energy minima located on the potential energy surface of the [(P<sup>N</sup>)Au(styrene)]<sup>+</sup> complex **1**. Bond distances in Å, relative energies from the ground-state structure **1** in kcal mol<sup>−1</sup> (ΔG values, with ΔE values in brackets). Calculations performed at the SMD-(dichloromethane)-B3PW91/SDD+f(Au),6-31G\*\* (other atoms) level of theory.



**Table 3** Optimized structures of the  $\pi$ -alkene gold(I) complexes **1–3** and **5–7** (bond lengths in Å). CDA, AIM, NBO analyses and charge transfer (Hirshfeld charges) from the alkene to the gold fragment

|   |  |  |  |  |  |  |  |
|---|---|---|---|---|--|---|---|
| <b>Geometrical parameters</b>                                     |   |   |   |   |  |   |   |
| Au–C  | 2.219   | 2.156   | 2.159   | 2.158   | 2.171  | 2.157   |   |
|   | 2.371   | 2.245   | 2.215   | 2.151   | 2.122  | 2.128   |   |
| $\Delta(\text{Au–C})^a$   | 0.152   | 0.089   | 0.056   | 0.007   | 0.049  | 0.029   |   |
| C=C   | 1.394   | 1.404   | 1.402   | 1.406   | 1.417  | 1.421   |   |
| (C=C olefin)  | (1.339)   | (1.339)   | (1.334)   | (1.331)   | (1.335)  | (1.334)   |   |
| $\Delta(\text{C=C})^b$  | 0.055   | 0.065   | 0.068   | 0.075   | 0.082  | 0.087   |   |
| Au–N  | 2.688   | 2.456   | 2.457   | 2.360   | 2.333  | 2.269   |   |
| <b>NBO analysis</b>   |   |   |   |   |  |   |   |
| WBI(C=C) <sup>c</sup>   | 1.477   | 1.475   | 1.501   | 1.489   | 1.437  | 1.341   |   |
| $\pi_{\text{CC}} \rightarrow \text{LP}^*(\text{Au})^d$            | 119.8   | 143.7   | 158.2   | 175.0   | 168.1  | 178.3   |   |
| $\text{LP}(\text{Au}) \rightarrow \pi_{\text{CC}}^*$ <sup>d</sup> | 23.0  | 36.7  | 38.9  | 45.1  | 45.1   | 48.9  |   |
| WBI(Au–N) <sup>c</sup>  | 0.048   | 0.085   | 0.093   | 0.125   | 0.138  | 0.167   |   |
| $\text{LP}(\text{N}) \rightarrow \text{Au}^d$                     | 10.8  | 20.0  | 22.0  | 32.4  | 34.0   | 44.0  |   |
| <b>CDA analysis</b>   |   |   |   |   |  |   |   |
| $d(\text{CC} \rightarrow \text{Au})^e$                            | 0.411   | 0.416   | 0.529   | 0.477   | 0.485  | 0.399   |   |
| $b(\text{Au} \rightarrow \text{CC})^e$                            | 0.146   | 0.211   | 0.230   | 0.262   | 0.274  | 0.323   |   |
| d/b   | 2.82  | 1.97  | 2.30  | 1.82  | 1.77   | 1.24  |   |
| <b>AIM analysis</b>   |   |   |   |   |  |   |   |
| $\rho(\text{C=C})^f$  | 0.313   | 0.305   | 0.307   | 0.303   | 0.297  | 0.297   |   |
| $\delta(\text{C=C})^f$  | 1.29  | 1.31  | 1.32  | 1.32  | 1.26   | 1.22  |   |
| $\rho(\text{Au–N})^f$   | 0.035   | 0.054   | 0.053   | 0.064   | 0.068  | 0.078   |   |
| $\delta(\text{Au–N})^f$   | 0.269   | 0.383   | 0.385   | 0.448   | 0.474  | 0.516   |   |
| <b>Hirshfeld charge</b>   |   |   |   |   |  |   |   |
| $\text{CT}(\text{CC} \rightarrow \text{Au})^g$                    | 0.16  | 0.06  | 0.05  | –0.003  | –0.06  | –0.12   |   |

<sup>a</sup> Difference between the two Au–C bond lengths. <sup>b</sup> Difference between C=C bond length in the gold complex and in the free alkene. <sup>c</sup> Bond indexes [WBI: Wiberg and  $\delta$ : Bader]. <sup>d</sup> Stabilizing energy  $\Delta E(2)$  at 2<sup>nd</sup> order perturbation theory in kcal mol<sup>–1</sup>. <sup>e</sup> Donation term (d) and back-donation term (b). <sup>f</sup> Density in e bohr<sup>–3</sup>. <sup>g</sup> Charge transfer (CT) from Hirshfeld charges.

interaction and N  $\rightarrow$  Au coordination. CDA indicates significant contribution of back-donation in **1** ( $d/b = 1.97$ ), much more than in the dicoordinate forms ( $d/b = 3.78$ ). This is in line with the in-plane arrangement of the alkene [the bent P–Au–N fragment formed by chelation features a high-energy occupied  $d(\text{Au})$  orbital of suitable geometry for back-donation to the  $\pi_{\text{C=C}}^*$  (alkene) orbital].<sup>13,15</sup> The  $\text{Au} \rightarrow \pi_{\text{C=C}}^*$  back-donation is also apparent in the NBO analysis as a donor–acceptor interaction with noticeable stabilizing energy (36.7 kcal mol<sup>–1</sup>). Consistently, the C=C double bond is substantially weakened upon coordination to gold, as apparent from the Wiberg bond index (WBI) at 1.475 in **1** (versus 1.900 in free styrene) and from the electron density at the bond-critical point (BCP)  $\rho(\text{C=C}) = 0.305$  au in **1** (versus 0.341 in free styrene). Back-donation roughly compensates donation so that overall, the alkene to gold charge transfer is small (0.06e as deduced from Hirshfeld charges). NBO and AIM also provide evidence for significant N  $\rightarrow$  Au interaction in **1**: a donor–acceptor interaction between N and Au is found at the second order perturbation level in NBO, with

a delocalization energy of 20 kcal mol<sup>–1</sup>, and a BCP with non-negligible electron density [ $\rho(\text{N–Au}) = 0.05$  au] is found in AIM.

**Other (P^N)Au(alkene)<sup>+</sup> complex: DHP, hex-1-ene, ethylene, MA and NPM.** The computational study was then extended to all the [(P^N)Au(alkene)]<sup>+</sup> complexes. Complete data are provided in the ESI:<sup>†</sup> optimized geometries of the ground-state and of isomers, bonding analyses *via* NBO, CDA and AIM. Only the key results are discussed here, in particular with regards to the impact of the alkene electronics on the Au/alkene interaction and the response of the P^N ligand (Table 3).

As for the styrene complex **1**, the alkene is in-plane side-on coordinated to gold and the P^N ligand is chelating. The ground-state structures correspond to those observed experimentally, and their optimized geometries reproduce well those determined crystallographically. All alkenes are coordinated to gold in a quasi-symmetric manner [ $\Delta(\text{Au–C}) \leq 0.056$  Å], the largest deviations between the two Au–C bond lengths being observed for styrene (0.089 Å) and for the electron-rich DHP (0.152 Å). Coordination of the alkene to gold induces noticeable



elongation of the C=C double bond, which increases from 0.055 Å for DHP, to 0.087 Å for NPM. The N–Au distance also varies significantly in the series (by about 20%, from 2.269 Å for NPM, to 2.688 Å for DHP), in line with that observed crystallographically.

CDA indicates marked differences in the Au/alkene interaction as well, with the d/b ratio varying from 2.8 for DHP to 1.2 for NPM. This evolution is mainly driven by the Au  $\rightarrow \pi_{\text{C}=\text{C}}^*$  back-donation term ( $\pi_{\text{C}=\text{C}} \rightarrow \text{Au}$  donation varies less), in line with the energy of the frontier molecular orbitals of the alkenes [the  $\pi(\text{C}=\text{C})$  orbital varies less in energy than the  $\pi^*(\text{C}=\text{C})$ , Fig. S32†]. The variation of the d/b ratio is accompanied by an inversion of the alkene  $\rightarrow \text{Au}$  charge transfer, from 0.16e for DHP to  $-0.12e$  for NPM. According to NBO and AIM, the weakening of the C=C double bond upon coordination to gold increases from electron-rich to electron-poor alkenes, consistent with the strengthening of Au  $\rightarrow \pi_{\text{C}=\text{C}}^*$  back-donation (and decrease of the d/b ratio): the Wiberg bond index decreases from 1.477 for DHP, to 1.341 for NPM, while the electron density at the bond-critical point  $\rho(\text{C}=\text{C})$  decreases from 0.313 (DHP) to 0.297 (NPM).

It is also noteworthy that the P<sup>^</sup>N ligand strongly responds to the electronic requirements at gold by strengthening/weakening the N  $\rightarrow$  Au coordination. The delocalization energy associated with the donor-acceptor interaction (as found in the NBO analysis) increases from 10.8 kcal mol<sup>-1</sup> for DHP, to 44.0 kcal mol<sup>-1</sup> for NPM. In parallel, AIM calculations

show an increase of the electron density at the bond critical point  $\rho(\text{N}-\text{Au})$  from 0.269 for DHP, to 0.516 for NPM.

### Parametrization of the P<sup>^</sup>N ligand response as a function of the alkene coordination to gold

Having in hand a range of experimental and theoretical data on a series of  $\pi$ -alkene complexes gave us the possibility to analyse in detail how the P<sup>^</sup>N ligand responds to the electronics of the alkene coordinated to gold. We looked in particular for correlations between the P<sup>^</sup>N ligand behaviour and the Au/alkene interaction.<sup>16</sup> Based on the previous detailed analyses, four descriptors were chosen to account for the P<sup>^</sup>N ligand coordination: the Au–N distance,<sup>17</sup> the <sup>1</sup>H NMR chemical shift of the NMe<sub>2</sub> group, the electron density at the N–Au bond critical point  $\rho(\text{N}-\text{Au})$  (AIM) and the <sup>31</sup>P NMR chemical shift. For the Au/alkene interaction, three parameters were used: the d/b ratio (CDA), the difference in the electron density at the C=C bond critical point between the coordinated and free alkene  $\Delta\rho(\text{C}=\text{C})$  (AIM) and the charge transfer from the alkene to the [(P<sup>^</sup>N)Au<sup>+</sup>] fragment (Hirshfeld charges).

A very similar and general trend is observed for all the examined sets of descriptors (Fig. 4): linear relationships are found between the P<sup>^</sup>N ligand behaviour and the alkene coordination to gold. Regression factors are generally above 0.92 and all are above 0.84. Most noteworthy is the intimate correlation between the strength of N  $\rightarrow$  Au coordination and the Au/alkene interaction. These linear correlations highlight the

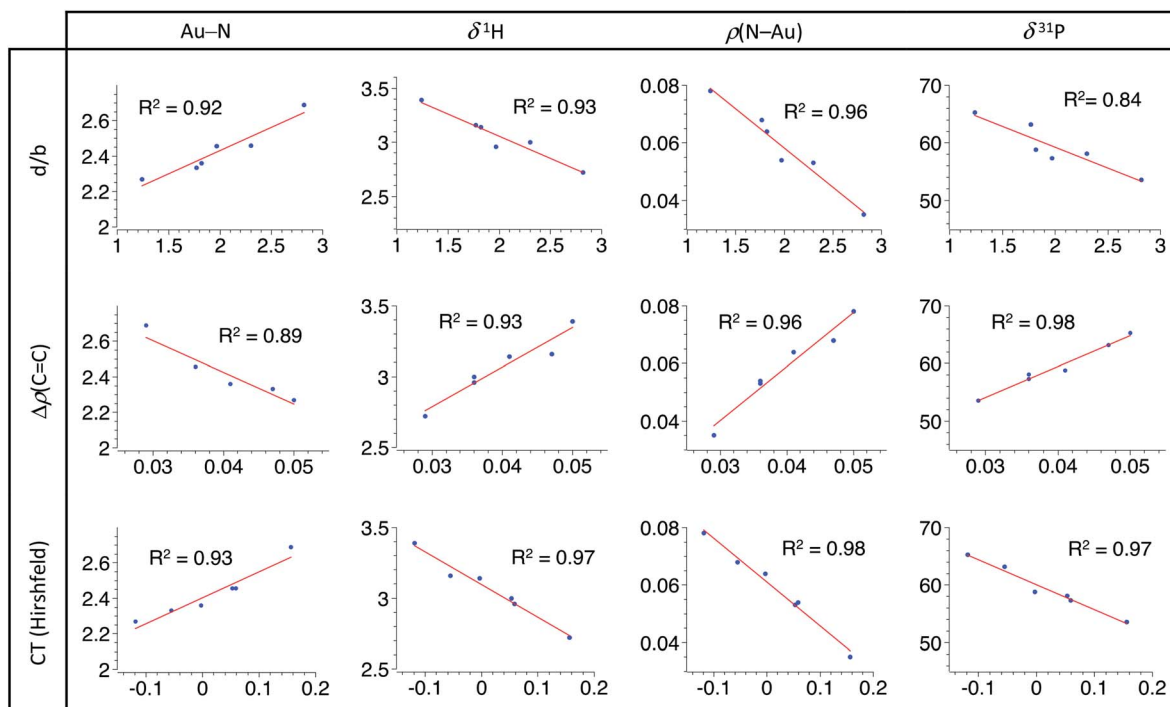


Fig. 4 Correlation graphs accounting for the response of the P<sup>^</sup>N ligand (as monitored by the N...Au bond length in Å, the <sup>1</sup>H NMR chemical shift of the NMe<sub>2</sub> group in ppm, the electron density at the N–Au bond critical point in au, the <sup>31</sup>P NMR chemical shift in ppm) to the alkene coordination to gold (as characterized by the d/b ratio, the difference in the electron density at the C=C bond critical point between the coordinated and free alkene in au, the charge transfer from the alkene to the [(P<sup>^</sup>N)Au<sup>+</sup>] fragment in e), including linear regressions and associated R-factors.





progressive response of the P<sup>^</sup>N ligand to the alkene electronics. Thanks to its hemilability, the P<sup>^</sup>N ligand displays non-innocent and adaptative character which is key to accommodate the  $\pi$ -coordination of a wide range of alkenes at gold, from electron-rich to electron-poor ones.

### Catalytic relevance of the (P<sup>^</sup>N)Au(I) $\pi$ -complexes

Finally, we sought to show that the gold(I)  $\pi$ -complexes isolated thanks to the P<sup>^</sup>N ligand exhibit reactivity typical of transient  $\pi$ -alkene gold(I) complexes and are catalytically relevant. To this end, the intermolecular hydroarylation of alkenes with indoles, as pioneered by M.-K. Wong and C.-M. Che,<sup>18</sup> was chosen.<sup>19</sup> In our previous study, MeDalphos gold(I) chloride was shown to catalyze the hydroarylation of styrene to give indoles **13a,b** and the role of the gold(I)  $\pi$ -complex as key intermediate was supported.<sup>10</sup> Here,  $\pi$ -systems with distinct electronic properties, MA and NPM as electron-poor alkenes and DHP as electron-rich alkene, were tested (Scheme 3).<sup>11</sup> In all cases, the hydroarylation reaction proceeded and complete selectivity for C3-alkylation of the indole was observed. The obtained compounds **13** result from nucleophilic attack of the indole to the most electrophilic position of the  $\pi$ -coordinated alkene, resulting in Markovnikov or anti-Markovnikov products depending on the substrate.<sup>20</sup> In the case of DHP, the double addition products **13e,f** were quantitatively obtained. They result from facile ring-opening of the first-formed hydroarylation product upon addition of

a second indole molecule.<sup>21</sup> The fate of the hydroarylation reaction of DHP was unambiguously established by using 6-nitroindole, for which the resulting product **13g** could be characterized by X-ray diffraction.<sup>11</sup>

## Conclusions

In summary, the P<sup>^</sup>N ligand MeDalphos was found to enable access to stable gold(I)  $\pi$ -complexes with a wide range of alkenes, from unbiased to electron-rich as well as electron-poor alkenes. Precedents of gold complexes deriving from electron-rich alkenes are rare,<sup>7</sup> and in the examples reported so far, the C=C bond tends to coordinate in a terminal or highly dissymmetric fashion. Here, dihydropyrene (DHP) was found to coordinate to the [(P<sup>^</sup>N)Au<sup>+</sup>] fragment more unsymmetrically than the other alkenes. Yet it remains side-on coordinated, with weakened but not negligible Au  $\rightarrow$  alkene back-donation. To the best of our knowledge, the methylacrylate (MA) and *N*-phenylmaleimide (NPM) adducts are the first examples of gold  $\pi$ -complexes with electron-poor alkenes.<sup>22</sup>

The P<sup>^</sup>N ligand displays adaptative character and accommodates the electron demand at gold as a function of the coordinated alkene by weakening/strengthening the N  $\rightarrow$  Au coordination. This “chameleon” behaviour enables to access stable  $\pi$ -complexes with various degrees of alkene  $\rightarrow$  Au donation/Au  $\rightarrow$  alkene back-donation, C=C bond weakening and alkene to gold charge transfer. Detailed examination of the structural, electronic and spectroscopic data collected experimentally and computationally for the series of  $\pi$ -complexes reveal direct and linear response of the P<sup>^</sup>N ligand to the Au/alkene coordination.

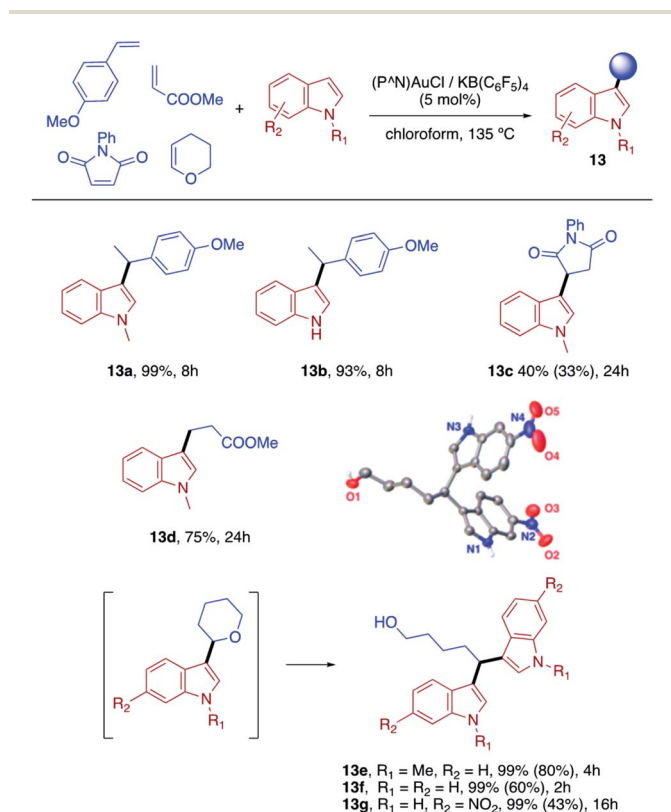
These results highlight a new feature of the MeDalphos ligand framework in gold chemistry, besides its ability to trigger Au(I)/Au(III) two-electron redox transformation<sup>13,23</sup> and to support hydrogen bonding to gold(I).<sup>24</sup> It is also noteworthy that the isolated P<sup>^</sup>N gold(I)  $\pi$ -complexes are reactive and amenable to catalysis, as substantiated by the chemo and regio-selective alkylation of indoles. The use of bidentate ligands in  $\pi$ -activation of alkenes at gold may be very interesting to circumvent the inherent difficulty associated with monodentate ligands and two-coordinate linear complexes when dealing with asymmetric catalysis using chiral ligands.<sup>25</sup>

## Conflicts of interest

There are no conflicts to declare.

## Acknowledgements

Financial support from the Centre National de la Recherche Scientifique and the Université de Toulouse is gratefully acknowledged. M. N. thanks the Fonds National Suisse de la Recherche Scientifique for an Early Postdoc Mobility fellowship. A. T. thanks Spanish MINECO for a mobility fellowship (BES-2014-067770 and EEBB-I-18-12874). S. Massou and P. Lavedan (ICT) are acknowledged for his assistance with NMR experiments. The “Direction du Numérique” of the Université de Pau



Scheme 3 Hydroarylation of alkenes with indoles catalyzed by the (P<sup>^</sup>N) gold(I) complex. Conversions determined by <sup>1</sup>H NMR spectroscopy; isolated yields after column chromatography in brackets. Crystallographic structure of compound **13g** as an insert.



et des Pays de l'Adour, MCIA (Mésocentre de Calcul Intensif Aquitain) and CINES under allocation A005080045 made by Grand Equipement National de Calcul Intensif (GENCI) are acknowledged for computational facilities.

## Notes and references

- 1 B. Hammer and J. K. Norskov, *Nature*, 1995, **376**, 238–240.
- 2 (a) G. Dyker, *Angew. Chem., Int. Ed.*, 2000, **39**, 4237–4239; (b) A. S. K. Hashmi, *Gold Bull.*, 2004, **37**, 51–65; (c) A. Hoffman-Röder and N. Krause, *Org. Biomol. Chem.*, 2005, **3**, 387–391; (d) A. S. K. Hashmi and F. D. Toste, *Modern Gold Catalyzed Synthesis*, Wiley-VCH, 2012; (e) D. Toste and V. Michelet, *Gold Catalysis: An Homogeneous Approach*, Imperial College Press, 2014; (f) L. M. Slaughter, *Homogeneous Gold Catalysis*, Springer, 2015.
- 3 (a) C. Winter and N. Krause, *Chem. Rev.*, 2011, **111**, 1994–2009; (b) M. Chiarucci and M. Bandini, *Beilstein J. Org. Chem.*, 2013, **9**, 2586–2614; (c) C. Obrados and A. M. Echavarren, *Chem. Commun.*, 2014, **50**, 16–28; (d) R. Doral and A. M. Echavarren, *Chem. Rev.*, 2015, **115**, 9028–9072; (e) C. J. V. Halliday and M. Lynam, *Dalton Trans.*, 2016, **45**, 12611–12626; (f) J. L. Mascareñas, I. Varela and F. López, *Acc. Chem. Res.*, 2019, **52**, 465–479.
- 4 (a) H. Schmidbaur and A. Schier, *Organometallics*, 2010, **29**, 2–23; (b) M. A. Cinellu in *Modern Gold Catalyzed Synthesis*, Wiley-VCH, Weinheim, 2012, pp. 175–199; (c) R. E. M. Brooner and R. A. Widenhoefer, *Angew. Chem., Int. Ed.*, 2013, **52**, 11714–11724; (d) A. C. Jones, *Top. Curr. Chem.*, 2015, **357**, 133–166.
- 5 (a) D. B. Dell'Amico, F. Calderazzo, R. Dantona, J. Strähle and H. Weiss, *Organometallics*, 1987, **6**, 1207–1210; (b) R. M. Davila, R. J. Staples and J. P. Fackler Jr, *Organometallics*, 1994, **13**, 418–420; (c) T. J. Brown, M. G. Dickens and R. A. Widenhoefer, *J. Am. Chem. Soc.*, 2009, **131**, 6350–6351; (d) T. N. Hooper, M. Green, J. E. McGrady, J. R. Patel and C. A. Russell, *Chem. Commun.*, 2009, 3877–3879.
- 6 Gold(III)  $\pi$  complexes are also known, but rare, see: (a) N. Salvjani, D. Rosca, M. Schormann and M. Bochmann, *Angew. Chem., Int. Ed.*, 2013, **52**, 874–877; (b) E. Langseth, M. L. Scheuermann, D. Balcells, W. Kaminsky, K. I. Goldberg, O. Eisenstein, R. H. Heyn and M. Tilset, *Angew. Chem., Int. Ed.*, 2013, **52**, 1660–1663; (c) C. Blons, A. Amgoune and D. Bourissou, *Dalton Trans.*, 2018, **47**, 10388–10393.
- 7 (a) A. Fürstner, M. Alcarazo, R. Goddard and C. W. Lehmann, *Angew. Chem., Int. Ed.*, 2008, **47**, 3210–3214; (b) R. A. Sanguramath, T. N. Hooper, C. P. Butts, M. Green, J. E. McGrady and C. A. Russell, *Angew. Chem., Int. Ed.*, 2011, **50**, 7592–7595; (c) Y. Zhu, C. S. Day and A. C. Jones, *Organometallics*, 2012, **31**, 7332–7335; (d) M. Sriram, Y. Zhu, A. M. Camp, C. S. Day and A. C. Jones, *Organometallics*, 2014, **33**, 4157–4164; (e) A. Zhdanko and M. E. Maier, *Angew. Chem., Int. Ed.*, 2014, **53**, 7760–7764.
- 8 (a) M. A. Cinellu, G. Minghetti, S. Stoccoro, A. Zucca and M. Manassero, *Chem. Commun.*, 2004, 1618–1619; (b) M. A. Cinellu, G. Minghetti, F. Cocco, S. Stoccoro, A. Zucca, M. Manassero and M. Arca, *Dalton Trans.*, 2006, 5703–5716; (c) J. Wu and H. V. R. Dias, *Angew. Chem., Int. Ed.*, 2004, **46**, 7814–7816; (d) J. A. Flores and H. V. R. Dias, *Inorg. Chem.*, 2008, **47**, 4448–4450; (e) H. V. R. Dias and J. Wu, *Organometallics*, 2012, **31**, 1511–1517; (f) S. G. Ridlen, J. Wu, N. V. Kulkarni and H. V. R. Dias, *Eur. J. Inorg. Chem.*, 2016, 2573–2580; (g) K. Klimovica, K. Kirschbaum and O. Daugulis, *Organometallics*, 2016, **35**, 2938–2943; (h) M. J. Harper, C. J. Arthur, J. Crosby, E. J. Emmet, R. L. Falconer, A. J. Fensham-Smith, P. J. Gates, T. Leman, J. E. McGrady, J. F. Bower and C. A. Russell, *J. Am. Chem. Soc.*, 2018, **140**, 4440–4445; (i) Y. Yang, P. Antoni, M. Zimmer, K. Sekine, F. F. Mulks, L. Hu, L. Zhang, M. Rudolph, F. Rominger and A. S. K Hashmi, *Angew. Chem., Int. Ed.*, 2019, **58**, 5129–5133.
- 9 M. A. Gimeno and A. Laguna, *Chem. Rev.*, 1997, **97**, 511–522.
- 10 M. Navarro, A. Toledo, M. Joost, A. Amgoune, S. Mallet-Ladeira and D. Bourissou, *Chem. Commun.*, 2019, **55**, 7974–7977.
- 11 See the ESI for details.†
- 12 Only one form is found for the non-symmetric complexes **1**, **5** and **6**. The Ph groups of styrene and the O atom of DHP sit in the *cis* position to the PAD<sub>2</sub> group in **1** and **5**, while the CO<sub>2</sub>Me group of MA sits in the *cis* position to the NMe<sub>2</sub> group in **6**. These are also the only forms present in solution for complexes **1** and **6**, as supported by <sup>1</sup>H–<sup>15</sup>N HSQC NMR experiments.<sup>11</sup>
- 13 We have previously shown that the MeDalphos ligand enables oxidative addition to gold and promote Au(I)/Au(III) cycling thanks to its hemilabile character: (a) A. Zeineddine, L. Estévez, S. Mallet-Ladeira, K. Miqueu, A. Amgoune and D. Bourissou, *Nat. Commun.*, 2017, **8**, 565–572; (b) J. Rodríguez, A. Zeineddine, E. D. Sosa-Carrizo, K. Miqueu, N. Saffon-Merceron, A. Amgoune and D. Bourissou, *Chem. Sci.*, 2019, **10**, 7183–7192.
- 14 M. A. Cinellu, M. Arca, F. Ortu, S. Stoccoro, A. Zucca, A. Pintus and L. Maiore, *Eur. J. Inorg. Chem.*, 2019, 4784–4795.
- 15 (a) M. Joost, A. Zeineddine, L. Estévez, S. Mallet-Ladeira, K. Miqueu, A. Amgoune and D. Bourissou, *J. Am. Chem. Soc.*, 2014, **136**, 14654–14657; (b) M. Joost, L. Estévez, S. Mallet-Ladeira, K. Miqueu, A. Amgoune and D. Bourissou, *Angew. Chem., Int. Ed.*, 2014, **53**, 14512–14516; (c) M. Joost, L. Estévez, K. Miqueu, A. Amgoune and D. Bourissou, *Angew. Chem., Int. Ed.*, 2015, **54**, 5236–5240.
- 16 For recent reviews on parametrizing ligand properties and interrogation of structure/function relationship in transition metal chemistry, see: (a) M. S. Sigman, K. C. Harper, E. N. Bess and A. Milo, *Acc. Chem. Res.*, 2016, **49**, 1292–1301; (b) D. J. Durand and N. Fey, *Chem. Rev.*, 2019, **119**, 6561–6594.
- 17 The value for the DFT-optimized structure was used for all complexes so that the correlation covers all alkenes, including hex-1-ene.
- 18 M.-Z. Wang, M.-K. Wong and C.-M. Che, *Chem.–Eur. J.*, 2008, **14**, 8353–8364.



- 19 For a review on gold-catalyzed functionalization of indoles, see: V. Pirovano, *Eur. J. Org. Chem.*, 2018, 1925–1945.
- 20 For a recent theoretical study of the regioselectivity of nucleophilic addition to dicoordinate  $\pi$ -alkene gold(I) complexes, see: A. Couce-Rios, A. Lledós, I. Fernández and G. Ujaque, *ACS Catal.*, 2019, 9, 848–858.
- 21 J. S. Yadav, B. V. S. Reddy, G. Satheesh, A. Prabhakar and A. C. Kunwar, *Tetrahedron Lett.*, 2003, 44, 2221–2224.
- 22 For gold-catalyzed transformations involving electron-poor alkenes as substrates, see: (a) F. Medina, C. Michon and F. Agbossou-Niedercorn, *Eur. J. Org. Chem.*, 2012, 6218–6227; (b) V. Pirovano, D. Facoetti, M. Dell'Acqua, E. Della Fontana, G. Abbiati and E. Rossi, *Org. Lett.*, 2013, 15, 3812–3815; (c) X. Hu, D. Martin, M. Melaimi and G. Bertrand, *J. Am. Chem. Soc.*, 2014, 136, 13594–13597.
- 23 (a) M. O. Akram, A. Das, I. Chakrabarty and N. T. Patil, *Org. Lett.*, 2019, 21, 8101–8105; (b) J. Rodríguez, N. Adet, N. Saffon-Merceron and D. Bourissou, *Chem. Commun.*, 2020, 56, 94–97.
- 24 (a) M. Rigoulet, S. Massou, E. D. Sosa Carrizo, S. Mallet-Ladeira, A. Amgoune, K. Miqueu and D. Bourissou, *Proc. Natl. Acad. Sci. U. S. A.*, 2019, 116, 46–51; (b) H. Schmidbaur, *Angew. Chem., Int. Ed.*, 2019, 58, 5806–5809.
- 25 (a) F. López and J. L. Mascareñas, *Beilstein J. Org. Chem.*, 2013, 9, 2250–2264; (b) Y.-M. Wang, A. D. Lackner and F. D. Toste, *Acc. Chem. Res.*, 2014, 47, 889–901; (c) W. Zi and F. D. Toste, *Chem. Soc. Rev.*, 2016, 45, 4567–4589; (d) Y. Li, W. Li and J. Zhang, *Chem.–Eur. J.*, 2017, 23, 467–512; (e) J. Rodríguez and D. Bourissou, *Angew. Chem., Int. Ed.*, 2018, 57, 386–388.

